Antitumor Actinopyranones Produced by Streptomyces albus POR-04-15-053 Isolated from a Marine Sediment

ARTICLE *in* JOURNAL OF NATURAL PRODUCTS · JUNE 2011

Impact Factor: 3.8 · DOI: 10.1021/np200196j · Source: PubMed

JOURNAL OF NATURAL PRODUCTS

ARTICLE

pubs.acs.org/jnp

Antitumor Actinopyranones Produced by *Streptomyces albus* POR-04-15-053 Isolated from a Marine Sediment

Carmen Schleissner, Marta Pérez, Alejandro Losada, Pilar Rodríguez, Cristina Crespo, Paz Zúñiga, Rogelio Fernández, Fernando Reyes,[†] and Fernando de la Calle*

Drug Discovery Area, PharmaMar SAU, Avenida de los Reyes 1, 28770-Colmenar Viejo, Madrid, Spain[†]Fundación Medina, Granada, Spain.

Supporting Information

ABSTRACT:

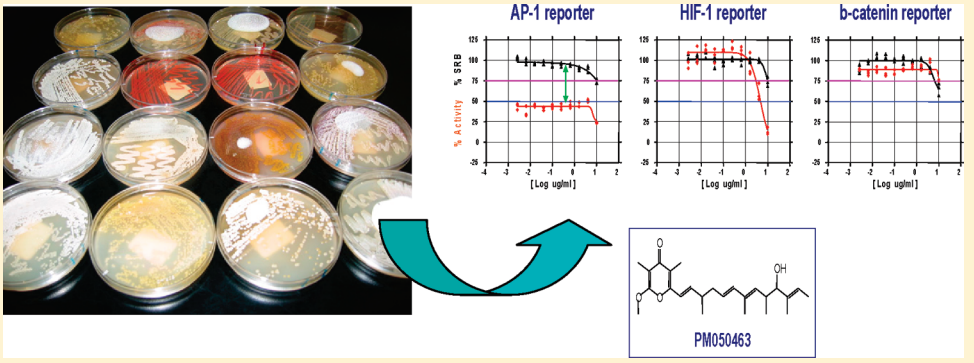

Four new antitumor pyranones, PM050511 (**1**), PM050463 (**2**), PM060054 (**3**), and PM060431 (**4**), were isolated from the cell extract of the marine-derived *Streptomyces albus* POR-04-15-053. Their structures were elucidated by a combination of spectroscopic methods, mainly 1D and 2D NMR and HRESIMS. They consist of an α-methoxy-γ-pyrone ring containing a highly substituted tetraene side chain glycosylated at C-10 in the case of **1** and **4**. Compounds **1** and **4** displayed strong cytotoxicity against three human tumor cell lines with GI_{50} values in the submicromolar range, whereas **2** showed subnanomolar activity as an inhibitor of EGFR-MAPK-AP1-mediated mitogenic signaling, causing inhibition of EGF-mediated AP1 trans-activation and EGF-mediated ERK activation and slight inhibition of EGF-mediated JNK activation. Taken together, these results suggest that members of the pyranone family of compounds could be developed as potential antitumor agents.

Pyranones are chemical structures isolated mainly from microorganisms and marine mollusks. These compounds have been disclosed to possess diverse biological activities. Actinopyrones A−C have been isolated from cultures of several *Streptomyces* species and have shown weakly antimicrobial and coronary vasodilating activities.[1] Structurally related metabolites, piericidins and glucopiericidins, have also been found in *Streptomyces* cultures. Piericidins A and B were published as insecticides and mild antimicrobials.[2] Glucopiericidins have shown more potent antimicrobial and cytotoxic activities and *in vitro* inhibitory effects against antibody formation, although the acute toxicity of these substances in mice was lower than that of piericidin A.[3] Other pyranones such as lagunapyrones A−C, isolated from a marine sediment bacterium, were reported as cytotoxic acetogenins,[4] and verticipyrone, a NADH-fumarate reductase inhibitor, was obtained from the culture broth of the fungal strain *Verticillium* sp. FKI-1083.[5]

In addition, extracts of marine mollusks, such as the air-breathing gastropod *Siphonaria diemensis*,[6] have been the source of the antimicrobials dimenensins A and B, and peptinatones, isolated from *S. grisea*[7] *and S. pectinata*, have shown mild *in vitro* antitumor activities.[8] Finally, fusaripyrones A and B, polypropionates isolated from the Mediterranean pulmonate mollusk *Haminoea fusari*, displayed antifouling activity but no general toxicity.[9]

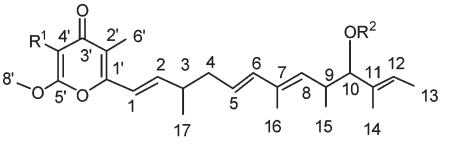

1: R^1 = Me, R^2 = X
2: R^1 = Me, R^2 = H
3: R^1 = Et, R^2 = H
4: R^1 = Et, R^2 = X

RESULTS AND DISCUSSION

In our effort to search for new antitumor compounds from marine microorganisms, we have isolated four α-methoxy-γ-pyrones containing highly substituted tetraene side chains,

Received: March 2, 2011
Published: June 30, 2011

Table 1. ^{1}H and ^{13}C NMR (CD_3OD, 500 and 125 MHz) and HMBC Assignments of 1 and 2

	1			2		
position	δ_C	δ_H, mult. (J in Hz)	HMBC[a]	δ_C	δ_H, mult. (J in Hz)	HMBC[a]
1	119.1	6.49, d (15.5)	1′, 2, 3	119.0	6.49, d (15.5)	1′, 2, 3
2	145.1	6.57, dd (15.5, 7.5)	1′, 1	145.1	6.57, dd (15.5, 8.0)	1′, 1
3	38.9	2.52, m	1, 2, 4, 5, 17	38.8	2.53, m	1, 2, 4, 5, 17
4	41.0	2.23, m	2, 3, 5, 6, 17	41.1	2.25, m	2, 3, 5, 6, 17
5	125.8	5.57, ddd (15.0, 7.5, 7.5)	4, 7	125.6	5.57, ddd (15.0, 7.5, 7.5)	4, 7
6	138.3	6.12, d (15.0)	4, 7, 8, 16	138.5	6.12, d (15.0)	4, 8, 16
7	134.5			134.8		
8	136.2	5.41, d (9.5)	6, 15, 16	135.9	5.30, d (9.5)	6, 16
9	36.9	2.77, m	7, 11, 15	37.6	2.67, m	8, 10, 15
10	93.6	3.72, d (8.5)	1″, 9, 11, 12, 14, 15	83.7	3.69, d (8.5)	8, 9, 12, 14
11	137.0			138.1		
12	124.3	5.45, m	10, 13, 14	122.7	5.43, m	10, 13, 14
13	13.1	1.60, s	11, 12	13.1	1.74, s	11, 12
14	11.8	1.60, s	10, 11, 12	11.2	1.74, s	10, 11, 12
15	17.8	0.82, d (7.0)	8, 9, 10	18.2	0.81, d (7.0)	8, 9, 10
16	13.2	1.73, d (1.0)	6, 7, 8	13.1	1.82, s	6, 7, 8
17	19.8	1.14, d (7.0)	2, 3, 4	19.9	1.14, d (7.0)	2, 3, 4
1′	154.4			154.4		
2′	118.3			118.3		
3′	183.3			183.3		
4′	100.1			100.1		
5′	164.3			164.2		
6′	9.6	1.99, s	1′, 2′, 3′	9.6	2.04, s	1′, 2′, 3′
7′	7.1	1.82, s	3′, 4′, 5′	7.1	1.99, s	3′, 4′, 5′
8′	56.6	4.07, s	5′	56.6	4.07, s	5′
1″	104.2	4.20, d (8.0)	10			
2″	75.6	3.13, m				
3″	78.3	3.28, m	2″, 4″			
4″	71.6	3.26, m	2″, 3″			
5″	77.8	3.10, m				
6″	62.8	3.61, dd (12.0, 5.0)				
		3.73, dd (12.0, 3.0)				

[a] HMBC correlations are from proton (s) stated to the indicated carbon.

PM050511 (**1**), PM050463 (**2**), PM060054 (**3**), and PM060431 (**4**). This family of substances was obtained from cell extracts of the marine-derived actinomycete *Streptomyces albus* POR-04-15053, isolated from a marine sediment collected in the west-southern coast of the Iberian peninsula. The active compounds were obtained from the 2-propanol−EtOAc extract of the microorganism cells of a 6 L culture by bioassay-guided fractionation, employing reversed-phase VLC and semipreparative HPLC, to yield **1** (2 mg), **2** (2.5 mg) **3** (0.8 mg), and **4** (0.7 mg).

PM050511 (**1**) was isolated as a brownish oil soluble in common organic solvents such as MeOH and $CHCl_3$. Its molecular formula was established as $C_{31}H_{46}O_9$ by (+)-HRESIMS and ^{13}C NMR. Peaks at m/z 563 $[M + H]^+$, 585 $[M + Na]^+$, and 383 $[M - C_6H_{12}O_6 + H]^+$, the latter due to the loss of a sugar moiety, were found in the low-resolution ESI mass spectrum of the compound. Its IR spectrum indicated the presence of hydroxy groups (3406 cm^{-1}), unsaturated bonds (824 and 964 cm^{-1}), and α, β, α′, β' conjugated ketone (1661 cm^{-1}) functionalities.

The ^{13}C NMR spectrum (Table 1) of **1** showed 31 signals assigned to eight methyl, two methylene, 14 methine, and seven quaternary carbons by HSQC experiments. Its COSY spectrum revealed the connectivities from H-1 to H-6, from H-8 to H-10, and from H-12 to H_3-13 and identified fragments **B** to **D** in the molecule (Figure 2). The precise connectivity of **1** was established by interpretation of the HMBC data summarized in Table 1. HMBC correlations from the methoxy group H-8′ to C-5′, H_3-7′ to C-3′, C-4′, and C-5′, and H_3-6′ to C-1′ and C-3′ indicated the presence of the α-methoxy-γ-pyrone ring A in the structure of **1** (Figure 1). Furthermore, when comparing the ^{1}H and ^{13}C NMR data of **1** with those of actinopyrone A, a closely related structure,[1] the presence of the same α-methoxy-γ-pyrone ring in both substances was evident.

The nature of the side chain attached to C-1′ was deduced from HMBC correlations. A long-range coupling from H-1 and H-2 to C-1′ corroborated the linkage of the pyrone ring **A** to the aliphatic chain at C-1 in fragment **B**. In addition, long-distance correlations between H-5 and C-7, between H-6 and C-7 and C-8, and between H-8 and C-6 linked fragment **B** to **C**, and fragments **C** and **D** were coupled on the basis of HMBC cross-peaks between H-9 and C-11, H-10 and C-14, and H-12 and

dx.doi.org/10.1021/np200196j |J. Nat. Prod. 2011, 74, 1590–1596

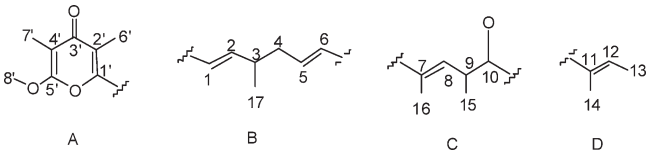

Figure 1. Partial structures determined for **1** in CD_3OD.

H_3-14 with C-10. Other long-distance correlations between H-1 and C-3, H_3-17 and H-4 with C-2, H-6 with C-4, H_3-15 with C-8, and H_3-13 with C-11 corroborated the structure proposed for **1**. The *E* configurations of the Δ^1 and Δ^6 double bonds were supported by coupling constants J_{1-2} and J_{5-6} of 15.5 and 16.0 Hz, respectively, and NOESY correlations observed between H-6 and H-8 and between H-10 and H-12 were in favor of the *E* configuration for both the Δ^7 and Δ^{11} double bonds.

The presence of a glycopyranosyl moiety in the structure was inferred from signals in the ^1H and ^{13}C spectra at δ_H/δ_C 4.20/104.2 (C-1″), 3.13/75.6 (C-2″), 3.28/78.3 (C-3″), 3.26/71.6 (C-4″), 3.10/77.8 (C-5″), and 3.61; 3.73/62.8 (C-6″) and couplings observed in the COSY and HMBC spectra (Table 1). The large $^1H-^1H$ coupling constant for H-1″ (8.0 Hz) indicated a β-glycoside configuration, as in the case of the glucopiericidins.[3] The long-range H−C coupling of the anomeric proton H-1″ with C-10 in the HMBC experiment suggested the linkage of the sugar moiety to this carbon of the side chain, corroborated by the presence of a cross-peak between H-1″ and H-10 in the ROESY spectrum. Finally, the identity of the sugar moiety, D-glucose, was confirmed by cross-peaks observed in the ROESY spectrum between H-1″ and H-3″ and H-5″ and hydrolysis of **1** in 1 N HCl at 80 °C followed by enantioselective GC analysis of the crude product (see Experimental Section).

Compound **2** was isolated as a white solid sensitive to air oxidation. The molecular formula of **2** was established as $C_{25}H_{36}O_4$ by positive HRESIMS. ^1H and ^{13}C NMR data (Table 1) confirmed compound **2** to be the aglycone moiety of **1**. Correlations observed in the COSY and HMBC spectra (Table 1) supported the proposed structure.

The absolute configuration at C-10 in **2** was assigned by application of the modified Mosher method.[10] Mosher acylation of **2** with both *S*- and *R*-MTPA chloride yielded the C-10 *R*- and *S*-α-methoxy-α-(trifluoromethy)phenyl acetyl (MTPA) esters. ^1H NMR data of the two isomers **2a** and **2b** are reported in the Supporting Information (S13). Analysis of the $\Delta\delta_{S-R}$ values on each side of the C-10 stereogenic center (Figure 2) suggested its *R* configuration, in spite of the anomalous positive value for H-12. On the other hand, a large coupling constant (8.5 Hz) revealed an *anti* relationship between H-9 and H-10, as observed in the case of piericidins.[11] A ROESY correlation between H_3-15 and H_3-14 established an *erythro* configuration between stereocenters C-9 and C-10 and therefore an *R* configuration for C-9. The absolute configuration at the C-3 asymmetric center remained to be determined.

Compound **3** was isolated as a brownish oil. Its molecular formula was established as $C_{26}H_{38}O_4$ by (+)-HRESIMS. Its ^1H NMR spectrum (Table 2) was very similar to that of **2**, with the most evident differences being the absence of the signal at δ 1.99 (H_3-7′) in **2**, replaced by the resonances for an ethyl group at δ 2.37 (q, 2H) and 1.00 (t, 3H) in the spectrum of **3**. Similar changes have been described for the spectra of the structurally related actinopyrones A and C[1] and corroborate the structure proposed for PM060054.

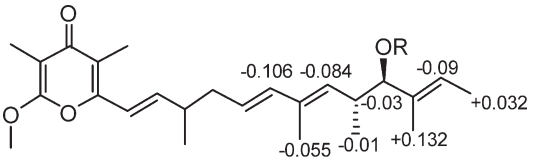

2a: R= (*R*)-MTPA
2b: R= (*S*)-MTPA

Figure 2. $\Delta\delta_{S-R}$ values for the C-10 Mosher esters **2a** and **2b** of PM050463 (**2**).

Table 2. ^1H NMR (CD_3OD, 500 MHz) Assignments for 3 and 4

	3	4
position	δ_H, mult. (*J* in Hz)	δ_H, mult. (*J* in Hz)
1	6.47, d (15.5)	6.49, d (15.5)
2	6.56, dd (15.5, 7.0)	6.57, dd (15.5, 7.0)
3	2.52, m	2.53, m
4	2.24, m	2.24, m
5	5.56, ddd (15.0, 7.5, 7.5)	5.58, ddd (15.0, 7.5, 7.5)
6	6.11, d, (15.0)	6.14, d (15.0)
7		
8	5.29, d (9.0)	5.41, d (9.5)
9	2.66, m	2.78, m
10	3.68, d (7.5)	3.73, d (8.5)
11		
12	5.42, m	5.46, m
13	1.60, s	1.61, s
14	1.58, s	1.61, s
15	0.80, d (6.5)	0.83, d (7.0)
16	1.73, d (1.0)	1.74, s
17	1.13, d (7.0)	1.14, d (7.0)
6′	1.97, s	1.99, s
7′	2.37, q (7.5)	2.39, q (8.0)
8′	1.00, t (7.0)	1.02, t (7.5)
9′	4.06, s	4.08, s
1″		4.21, d (7.5)
2″		3.15, m
3″		3.28, m
4″		3.26, m
5″		3.11, m
6″		3.62, dd (11.5, 5.0)
		3.74, m

Compound **4** was isolated as a brownish oil. Its molecular formula was established as $C_{32}H_{48}O_9$ by positive HRESIMS. When comparing the ^1H NMR spectrum of **4** (Table 2) with that of **1**, two new signals at δ 2.39 (q, 2H) and δ 1.02 (t, 3H) were observed for **4** instead of the signal at δ 1.82 (s, 3H) assigned to the methyl group at the C-4′ carbon in **1**. These changes were in agreement with the replacement of the methyl group at C-4′ for an ethyl chain in **4**.

The cytotoxic activity of compounds **1**−**4** (Table 3) was tested against a panel of three human tumor cell lines representative of different tumor types, including breast (MDA-MB-231),

Table 3. Cytotoxic Activity Data (μM) of Compounds 1−4

		compound				control
cell line		1	2	3	4	doxorubicin hydrochloride
breast	GI_{50}	0.50	10.5	>22	0.24	0.09
MDA-MB-231	TGI	0.69	>22	>22	0.43	0.18
	LC_{50}	1.01	>22	>22	0.82	0.41
colon HT29	GI_{50}	0.69	10.8	21.5	0.38	0.15
	TGI	0.12	10.8	>22	1.23	0.18
	LC_{50}	0.24	11.5	>22	4.68	0.24
NSCLC A549	GI_{50}	0.53	5.00	18.6	0.28	0.06
	TGI	0.76	13.5	>22	0.52	0.20
	LC_{50}	1.16	>22	>22	1.08	0.59

Table 4. RTK (AP-1), HIF-1α, and β-Catenin Activity Data (IC_{50} in μM) of Compounds 1 and 2

	RTK (AP1)[a]	HIF-1α[b]	β-catenin[c]
	cervix HeLa-AP1	cervix HeLa-HIF-1	colon SW480-TCF
PM050511 (1)	0.16	0.06	0.17
PM060463 (2)	<0.007	0.47	0.66

[a] IC_{50} value represents the compound concentration producing 50% inhibition of RTK (AP-1) activity as compared to that of untreated control cells. [b] IC_{50} value represents the compound concentration producing 50% inhibition of HIF-1α activity as compared to that of untreated control cells. [c] IC_{50} value represents the compound concentration producing a 50% inhibition of β-catenin activity as compared to that of untreated control cells.

colon (HT29), and lung (A549). Compounds **1** and **4** exhibited strong activity with GI_{50} values in the range 0.24 to 0.69 μM, whereas compounds **2** and **3** displayed only mild cytotoxicity, with GI_{50} values ranging from 5 to >22 μM. The presence of a glucose residue in glucoactinopyrone molecules **1** and **4** seemed therefore to be necessary for the cytotoxic activity of this family of compounds. Similar results have been found in the analysis of the cytotoxic properties of glucopiericidins.[3]

Compounds **1** and **2** were tested in our primary *in vitro* targeted cell based EGF receptor tyrosine kinase (RTK) assay, using HeLa cells stably transfected with a construct carrying an AP1-response element. Pretreatment of cells with compound **2** caused inhibition of EGF-induced AP1 activation. In this case, **2** exhibited very strong activity, with an IC_{50} value lower than 7 nM, in contrast to the glycosylated **1** (IC_{50} = 0.16 μM) (Table 4). As a specificity control we used two other reporter genes, hypoxia-induced factor 1 (HIF-1) and β-catenin, which are also involved in tumor progression. Pretreatment of cells with **2** resulted in no detectable effect in β-catenin and HIF-1 transactivation. Activity observed with **1** in the RTK, β-catenin, and HIF-1 assays is associated with the cytotoxic activity of the compound and, therefore, not relevant in terms of biological significance regarding these targets.

Epidermal growth factor (EGF) is one of the most important mitogens for many epithelial cells and promotes cell proliferation and differentiation.[12,13] Epidermal growth factor receptor (EGFR) is a ligand-activated receptor tyrosine kinase. Binding of EGF to the receptor triggers receptor dimerization, activation of receptor tyrosine kinase activity, autophosphorylation, and transduction of the mitogenic signals to the nucleus via mitogen-activated protein kinases (MAPK).[14] The MAPK family includes ERK (extracellular signal-regulated kinase), JNK (c-jun N-terminal protein kinase), and p38.

In order to determine the level at which compound **2** is acting on the RTK intracellular signaling pathway, we investigated its activity on the EGFR-MAPK signaling pathway. First, we determined the effects of **1**, **2**, and **3** on EGF-induced EGFR activation. Cell lysates were examined by Western immunoblotting with antibodies that recognize the phosphorylated form of EGFR. As shown in Figure 3, treatment of cells with EGF caused a strong activation of EGFR; however, pretreatment of cells with tyrphostin AG1478, a highly potent and specific inhibitor of EGFR activation, resulted in a strong inhibition of EGF-induced EGFR activation. **2** did not modify EGFR autophosphorylation, indicating that it is acting downstream of this receptor.

EGF-induced activation of EGFR ultimately activates MAPK, which translocates to the nucleus and activates transcription factors (e.g., AP-1) for cell growth and proliferation.[12,13] We then tested the activation of ERK and JNK. Cells with or without preincubation with the compounds were treated with EGF, and cell lysates were examined by Western immunoblotting using phospho-ERK and phospho-JNK antibodies. As shown in Figure 3, pretreatment of cells with **2** produced a strong decrease in ERK phosphorylation and also a slight inhibition in JNK1 phosphorylation (upper band in the phospho-JNK row). Compound **2** also blocked EGF-mediated ERK activation after 4 h posttreatment (Figure 3). Reprobing blots with antibodies against total ERK2 and JNK1 revealed no change of protein levels upon treatments. Compounds **1** and **3** did not modify EGFR autophosphorylation. Compound **1** had no detectable effects on ERK and JNK activation, and **3** had no detectable effects on ERK, although it exerted a slight inhibition of JNK1 phosphorylation These experiments showed that **2** was acting at an intermediate step between EGFR and the MAPKs.

Activation of EGFR leads to the activation of Ras proteins, members of a superfamily of small GTP-binding proteins. Posttranslational modifications of Ras are required for their activation.[15] hRCE1 (human Ras-converting enzyme) is a prenyl protease that recognizes both farnesylated and geranylgeranylated Ras protein and removes the −AAX tripeptide in the cysteine residue of the farnesylated and geranylgeranylated c-terminus CAAX motif.[16] The modified Ras proteins are then translocated to the inner plasma membrane. Inhibition of Ras proteolysis by hCRE1 completely blocks Ras signaling. The activity of **2** as an inhibitor of EGFR-MAPK-AP1 could be similar to that published for the structurally related compounds barangcadoic acid A and the rhopaloic acids A, B, C, D, and E extracted from the marine sponge *Hippospongia* sp. These compounds inhibit the protease activity of hCRE1 and Ras signaling.[17]

In conclusion, marine-derived microorganisms can be a prolific source of target-directed natural product compounds, as in the case of PM050463 (**2**). Because most human tumors show mutations or alterations in Ras proteins, the inhibitory activity of compound **2** on the Ras-mediated signaling pathway, together with its cytotoxic action, could be of crucial interest for the development of this compound as an antitumor agent.

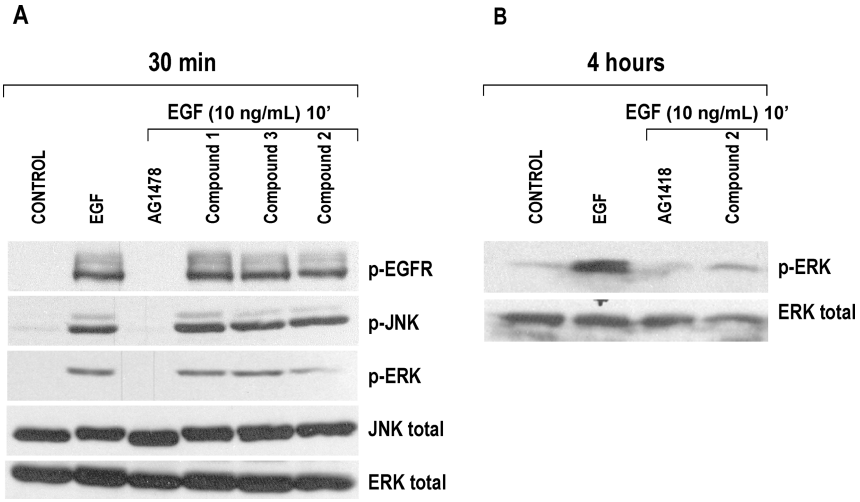

Figure 3. Effects of **2** on the phosphorylation of EGFR, ERK, and JNK. (A) Cells were preincubed with vehicle AG1478 as an inhibitor of EGFR activator or compounds **1**, **2**, and **3** for 30 min before treatment with EGF (10 min.). Phosphorylated forms of EGFR, JNK, and ERK were analyzed by Western blotting. Membranes were reprobed with antibodies against total JNK and ERK. (B) Cells were preincubed with vehicle, AG1478, or compound **2** for 4 h before treatment with EGF (10 min.). The phosphorylated form of ERK was analyzed by Western blotting. The membrane was reprobed with antibody against total ERK.

EXPERIMENTAL SECTION

General Experimental Procedures. Optical rotations were determined using a Jasco P-1020 polarimeter. UV spectra were obtained with an Agilent 8453. NMR spectra were recorded on a Varian "Unity 500" spectrometer at 500/125 MHz (^{1}H/^{13}C). Chemical shifts were reported in ppm using residual CD_3OD (δ 3.31 for ^{1}H and 49.0 for ^{13}C) as an internal reference. HMBC experiments were optimized for a $^3J_{CH}$ of 8 Hz. ROESY spectra were measured with a mixing time of 350 ms. (+)-HRESIMS was performed on a Applied Biosystems 4700 Proteomics Analyzer spectrometer. ESIMS were recorded using an Agilent 1100 Series LC/MSD spectrometer. GC analysis was carried out on an Agilent gas chromatograph using a HP-Chiral column (30 m × 0.25 mm, 0.25 μm); injection volume, 0.4 μL; detector temperature, 250 °C; injection temperature, 250 °C; injection mode: split (20:1) at constant 20 psi and 200 °C; carrier gas, He.

Isolation and Taxonomy of the Producer Microorganism. *Streptomyces albus* POR-04-15-053 was isolated from a suspension of marine sediment, collected in August 2004 by scuba at a depth 25 m at Punta Sagres (Portugal). A 2 mL sample of sediment gravel material was frozen at −20 °C for 96 h, and then 100 μL was seeded on Bennett's agar medium[18] plates supplemented with nalidixic acid (0.02%) and cycloheximide (0.02%). Plates were incubated at 28 °C for 30 days. The strain was subjected to phylogenetic analysis by the CECT (Colección Española de Cultivos Tipo), based on 16S rRNA sequences analyzed by BLAST (Basic Local Alignment Search Tool) against the National Center for Biotechnology Information (NCBI) database. GenBank accession number JN012607 showed high identity with that of *Streptomyces* spp. such as *Streptomyces albus* subsp. *albus* strain JCM 4703 (773/775, 99.7%) (sequence HQ537062.1). A culture of the strain has been deposited by PharmaMar in the CECT under the accession number CECT 3381.

Fermentation. A seed culture was developed in two scale-up steps, first in 100 mL Erlenmeyer flasks containing 20 mL of seed medium and then 250 mL Erlenmeyer flasks with 50 mL of the same medium. The seed culture was grown on a medium containing dextrose (0.1%), soluble starch 2.4%, soy peptone 0.3%, yeast extract 0.5%, tryptone 0.5%, soya flour 0.5%, sodium chloride 0.54%, potassium chloride 0.02%, magnesium chloride 0.24%, sodium sulfate 0.75%, and calcium carbonate 0.4% in tap water and cultured at 28 °C on an orbital skaker (5 cm eccentricity, 220 rpm) for 72 h. For production 12.5 mL of the seed medium was transferred into (×4) 2000 mL Erlenmeyer flasks containing 250 mL of fermentation medium containing yeast extract 0.5%, soy peptone 0.1%, dextrose 0.5%, soya flour 0.3%, Glucidex (Roquette) 2%, sodium chloride 0.53%, potassium chloride 0.02%, magnesium chloride·$6H_2O$ 0.24%, sodium sulfate 0.75%, manganese sulfate·$4H_2O$ 0.00076%, cobalt chloride·$6H_2O$ 0.0001%, dipotassium phosphate 0.05%, and calcium carbonate 0.4%. The culture was grown at 28 °C using an orbital shaker (5 cm eccentricity, 220 rpm) for 5 days.

Extraction and Isolation of Compounds 1−4. A 6 L portion of fermentation broth was centrifuged, and the mycelial cake (111 g) was homogenized first with 2-propanol (222 mL) and then with EtOAc (333 mL). The mixture was filtered through a pad of Celite. The filtered organic extract was concentrated under reduced pressure, giving a brownish, oily residue (867 mg). The extract was subjected to reversed-phase vacuum chromatography by filter funnel on Poligoprep 100-50 C_{18} using H_2O−MeOH−CH_2Cl_2 mixtures as the eluting solvents. The cytotoxic activity was detected in fractions eluted with H_2O−MeOH (1:3) and MeOH. These fractions were pooled (36 mg), and further purification by semipreparative HPLC was performed at room temperature (Symmetry C_{18}, 7.8 × 150 mm, gradient CH_3CN−H_2O from 30% to 100% CH_3CN in 30 min, flow rate 3 mL/min, UV detection at 215 nm). Compounds **1** (2.0 mg, t_R = 13.8 min), **2** (2.5 mg, t_R = 24.3 min), and **3** (0.8 mg, t_R = 26.9 min) were obtained under these conditions. Compound **4** (0.7 mg, t_R = 10.7 min) was isolated following a similar procedure from a 50 L fermentation broth (64 g of cell extract).

*PM050511 (**1**):* brownish oil; $[\alpha]^{25}_D$ +11 (*c* 0.01, MeOH); λ_{max} (log ε) 226 (5.32), 276 (2.05) nm; IR (KBr) ν_{max} 3911, 2366, 1781, 824, 799 cm^{-1}; ^{1}H and ^{13}C NMR spectra (500 and 125 MHz, respectively), see Table 1; (+)-ESIMS *m*/*z* 563 $[M + H]^+$, 585 $[M + Na]^+$, and 383 $[M - C_6H_{12}O_6 + H]^+$; (+)-HRESIMS *m*/*z* 563.3263 (calcd for $C_{31}H_{46}O_9$, 563.3220).

*PM050463 (**2**):* white solid; $[\alpha]^{25}_D$ +19 (*c* 0.01, MeOH); λ_{max} (log ε) 226 (4.55), 276 (1.80) nm; ^{1}H and ^{13}C NMR spectra (500 and 125 MHz, respectively), see Table 1; (+)-ESIMS *m*/*z* 401 $[M + H]^+$; (+)-HRESIMS *m*/*z* 401.2682 (calcd for $C_{25}H_{36}O_4$, 401.2686).

*PM060054 (**3**):* brownish oil; $[\alpha]^{25}_D$ −5.8 (*c* 0.01, MeOH); λ_{max} (log ε) 225 (1.80), 275 (1.17) nm; ^{1}H NMR spectrum (500 MHz), see

Table 2; (+)-ESIMS m/z 415 $[M + H]^+$; (+)-HRESIMS m/z 415.2818 (calcd for $C_{26}H_{38}O_4$ 415.2842).

*PM060431 (**4**):* brownish oil; $[\alpha]^{25}_D$ +18 (c 0.01, MeOH); λ_{max} (log ε) 227 (1.83), 276 (0.69) nm; ^{1}H NMR spectrum (500 MHz), see Table 2; (+)-ESIMS m/z 577 $[M + H]^+$; (+)-HRESIMS m/z 577.3347 (calcd for $C_{32}H_{48}O_9$ 577.3371).

Preparation of Mosher Esters of PM050463 (2). One crystal of dimethylaminopyridine was added to 3 mg (0.0075 mmol) of compound **2** in 0.5 mL of anhydrous CH_2Cl_2 at room temperature (rt) followed by the addition of Et_3N (10 μL). The reaction mixture was stirred at rt for 30 min, and then 7 mg of (*R*)- or (*S*)-α-methoxy-α-trifluoromethyl-α-phenylacetic acid chloride was added and the resultant mixture was stirred for another 90 min under N_2. The reaction mixture was then diluted with 5 mL of CH_2Cl_2 and washed with 1 N HCl (3 mL) and saturated NaCl (5 mL). The organic phase was evaporated, and the residue was separated by HPLC (Symmetry C_{18}, 7.8 × 150 mm, gradient MeOH−H_2O from 80% to 100% of MeOH in 30 min, flow 3 mL/min) to yield the 10-(*R*-MTPA) ester of **2** (**2a**, 3.5 mg) starting from (*S*)-MTPA-Cl. The 10-(*S*-MTPA) ester of **2** (**2b**, 4 mg), obtained from reaction of **2** with (*R*)-MTPA-Cl, was purified in a similar manner (Symmetry C_{18}, 7.8 × 150 mm, gradient MeOH−H_2O from 70% to 100% of MeOH in 30 min, flow 3 mL/min).

*10-(R-MTPA) Ester of **2** (**2a**):* white solid; $[\alpha]^{25}_D$ +17.0 (c 0.01, MeOH); λ_{max} (log ε) 225 (2.28), 276 (0.90) nm; ^{1}H NMR spectrum (Supporting Information S13); (+)-ESIMS m/z 617 $[M + H]^+$.

*10-(S-MTPA) Ester of **2** (**2b**):* white solid; $[\alpha]^{25}_D$ +3.1 (c 0.01, MeOH); λ_{max} (log ε) 225 (3.98), 276 (1.56) nm; ^{1}H NMR spectrum (Supporting Information S13); (+)-ESIMS m/z 617 $[M + H]^+$.

Acid Hydrolysis of Compound 1. A solution of **1** (5 mg) in 1 N HCl (1 mL) was heated at 80 °C for 4 h. After this period, the reaction mixture was evaporated to dryness, and then the residue was diluted with H_2O (0.5 mL) and extracted with $CHCl_3$ (3 × 0.5 mL). The aqueous phase was evaporated to dryness *in vacuo* to give a sugar residue, which was dissolved in anhydrous pyridine and 0.2 mL of L-cysteine methyl ester hydrochloride (0.06 M). The mixture was stirred at 60 °C for 2 h; then 0.3 mL of HMDS−TMCS (hexamethyldisilazane−trimethylchlorosilane, 3:1) was added, and the mixture was stirred at 60 °C for another 1 h. The precipitate was removed by centrifugation, and the supernatant was concentrated under a N_2 stream. The residue was partitioned between *n*-hexane and H_2O (0.2 mL each), and the hexane layer was analyzed by GC. D-Glucose was detected by co-injection of the silylated sugar sample with standard D- and L-silylated glucose, giving a single peak at 41.73 min.

Evaluation of Cytotoxic Activity. A549 (ATCC CCL-185), lung carcinoma; HT29 (ATCC HTB-38), colorectal carcinoma; and MDA-MB-231 (ATCC HTB-26), breast adenocarcinoma cell lines were obtained from the ATCC. Cell lines were maintained in RPMI medium supplemented with 10% fetal calf serum, 2 mM L-glutamine, and 100 U/mL penicillin and streptomycin, at 37 °C and 5% CO_2. Triplicate cultures were incubated for 72 h in the presence or absence of test compounds (at 10 concentrations ranging from 10 to 0.0026 μg/mL). For quantitative estimation of cytotoxicity, the colorimetric sulforhodamine B (SRB) method was used.[19] Briefly, cells were washed twice with PBS, fixed for 15 min in 1% glutaraldehyde solution, rinsed twice in phosphate-buffered saline (PBS), and stained in 0.4% SRB solution for 30 min at room temperature. Cells were then rinsed several times with 1% acetic acid solution and air-dried. Sulforhodamine B was then extracted in 10 mM Trizma base solution, and the absorbance measured at 490 nm. Doxorubicin hydrochloride was used as positive control.

Using the mean ± SD of triplicate cultures, a dose−response curve was automatically generated using nonlinear regression analysis. Three reference parameters were calculated (NCI algorithm) by automatic interpolation: GI_{50} = compound concentration that produces 50% cell growth inhibition, as compared to control cultures; TGI = total cell growth inhibition (cytostatic effect), as compared to control cultures, and LC_{50} = compound concentration that produces 50% net cell killing (cytotoxic effect).

Activator Protein 1 (AP-1), Hypoxia-Induced Factor 1α (HIF-1α), and β-Catenin Assays. AP-1 and HIF-1α transactivation was evaluated using HeLa cells (ATCC # CCL-2) stably transfected with a construct carrying a AP1-response element (TRE) or HIF-response element (HRE) upstream of a luciferase coding region. β-Catenin transactivation was evaluated using SW-480 cells (colon adenocarcinoma, ATCC # CCL-228) stably transfected with a construct carrying a TCF/β-catenin response element regulating the expression of a luciferase *reporter* gene. HeLa-AP1 cells, HeLa-HIF cells, and SW-480 cells were preincubated for 1 h with the test compounds. Then HeLa-AP1 cells were stimulated with 10 ng/mL EGF and HeLa-HIF cells were stimulated with 50 μM deferoxamine. EGF increased luciferase activity 7- to 10-fold over control values, and deferoxamine increased luciferase activity 80- to 100-fold over control values. Luciferase enzyme activity was determined using the Promega Bright-glo assay kit following the manufacturer's instructions and a Wallac Microbeta 1450 plate reader. The IC_{50} value represents the compound concentration producing 50% inhibition of AP-1, HIF-1, or β-catenin transcriptional activity as compared to that of untreated control cells.

Western Blotting. Cells were washed in PBS, collected, and resuspended in lysis buffer (20 mM Tris-HCl (pH 7.5), 150 mM NaCl, 1% (v/v) Nonidet P-40, 2 mM EDTA, 1 mM PMSF, 10 μg/mL aprotinin, and 10 μg/mL leupeptin) and kept on ice for 15 min. Cell extracts were cleared by microcentrifugation at 14000*g* for 30 min at 4 °C. Equal amounts of extracts were redissolved in SDS−PAGE and electroblotted to activated PVDF membranes (Immobilon-P, Millipore) following standard techniques. Membranes were sequentially probed with primary and appropriate secondary (horseradish-peroxidase-conjugated) antibodies following the manufacturer's instructions. Antibody−antigen complexes were detected using enhanced chemiluminescence system (Amersham Biotech).

■ ASSOCIATED CONTENT

Supporting Information. ^{1}H and ^{13}C NMR spectra for compounds **1** and **2**. ^{1}H NMR spectra for **3** and **4**. COSY, HSQC, HMBC, and ROESY spectra, IR adsorption spectrum, and ES-MS spectrum for **1**. ^{1}H NMR data for **2a** and **2b**. Epidermal growth factor receptor (EGFR) signaling pathways. This material is available free of change via the Internet at http://pubs.acs.org.

■ AUTHOR INFORMATION

Corresponding Author

*Tel: +34 91 846 6027. Fax: +34 91 846 6001. E-mail: fdelacalle@pharmamar.com.

■ ACKNOWLEDGMENT

We gratefully acknowledge the help of our PharmaMar colleagues C. de Eguilior and S. Bueno for collecting the marine samples, L. F. García for the design of biological assays, S. Munt for the revision of the manuscript, S. González for the performance of NMR experiments, A. Velasco and A. Peñalver for the molecular characterization of the microbial strain, and J. Garcia for the scale-up of the microbial cultures and the recovery of the fermentation broths.

■ REFERENCES

(1) Yano, K.; Yokoi, K.; Sato, J.; Oono, J.; Kouda, T.; Ogawa, Y.; Nakashima, T. *J. Antibiot.* **1986**, *39*, 32–43.

(2) Tahakashi, N.; Suzuki, A.; Kimura, Y.; Miyamoto, S.; Tamura, S.; Mitsui, T.; Fukami, J. *J. Agric. Biol. Chem.* **1968**, *32*, 1113–1122.
(3) Matsumoto, M.; Mogi, K. I.; Nagaoka, K.; Ishizeki, S.; Kawahara, R.; Nakashima, T. *J. Antibiot.* **1987**, *40*, 149–156.
(4) Lindel, T.; Jensen, P. R.; Fenical, W. *Tetrahedron Lett.* **1996**, *37*, 1327–1330.
(5) Ui, H.; Shiomi, K.; Suzuki, H.; Hatano, H.; Morimoto, H.; Yamaguchi, Y.; Masuma, R.; Sunazuka, T.; Shimamura, H.; Sakamoto, K.; Kita, K.; Miyoshi, H.; Tomoda, H.; Omura, S. *J. Antibiot.* **2006**, *59*, 785–790.
(6) Hochlowski, J. E.; Faulkner, J. *Tetrahedron Lett.* **1983**, *24*, 1917–1920.
(7) Norte, M.; Cataldo, F.; González, A. G.; Rodríguez, M. L.; Ruiz-Pérez, C. *Tetrahedron* **1990**, *46*, 1669–1678.
(8) Paul, M. C.; Zubía, E.; Ortega, M. J.; Salvá, J. *Tetrahedron* **1997**, *53*, 2303–2308.
(9) Cutignano, A.; Blihoghe, D.; Fontana, A.; Villani, G.; d'Ippolito, G.; Cimino, G. *Tetrahedron* **2007**, *63*, 12935–12939.
(10) Ohtani, I.; Kusumi, T.; Kakisawa, Y. *J. Am. Chem. Soc.* **1991**, *113*, 4092–4096.
(11) Hayakawa, Y.; Shirasaki, S.; Kawasaki, T.; Matsuo, Y.; Adachi, K.; Shizuri, Y. *J. Antibiot.* **2007**, *60*, 201–203.
(12) Yarden, Y.; Sliwkowski, M. X. *Nat. Rev. Mol. Cell. Biol.* **2001**, *2*, 127–137.
(13) Schlessinger, J. *Cell* **2000**, *103*, 211–225.
(14) Riese, D. J.; Sterm, D. F. *Bioassays* **1998**, *220*, 41–48.
(15) Downward *J. Nat. Rev. Cancer* **2003**, *3*, 11–22.
(16) Otto, J. C.; Kim, E.; Young, S. G.; Casey, P. J. *J. Biol. Chem.* **1999**, *274*, 8379–8382.
(17) Craig, K. S.; Williams, D. E.; Hollander, I.; Frommer, E.; Mallon, R.; Collins, K.; Wojciechowicz, D.; Tahir, A.; Van Soest, R.; Andersen, R. J. *Tetrahedron Lett.* **2002**, *43*, 4801–4804.
(18) Atalas, R. M. In *Handbook of Microbiological Media*, 3rd ed.; CRC Press LLC: Boca Raton, FL, 2004; pp 205−206.
(19) Skehan, P.; Storeng, R.; Scudiero, D.; Monks, A.; McMahon, J.; Vistica, D.; Warren, J. T.; Bokesch, H.; Kenney, S.; Boyd, M. R. *J. Natl. Cancer Inst.* **1990**, *82*, 1107–1112.